EDDY-VISCOSITY AND SECOND-MOMENT MODELS OF FREE PREMIXED FLAME

by

Miroslav SIJERČIĆ and Žarko STEVANOVIĆ

Original scientific paper
UDC: 532.517.4:662.951.2=20
BIBLID: 0354–9836, *2* (1998), 1, 13–31

This paper deals with the comparison of the eddy-viscosity and second-moment approaches for turbulence modeling of premixed jet flames. In order to predict the specific features of axisymetrical reacting free jets, the modified C_D coefficient in k-ε turbulence model is proposed. Special attention is paid to the second-moment model (Reynolds-Stress Turbulence Model) concerning the prediction of anisotropy level and correlation coefficients of turbulent diffusion of scalar components. The models are used for prediction of premixed turbulent acetylene flame. Calculation results are compared with the experimental data. The qualitative and quantitative comparison between two approaches is presented. The results of these computations demonstrate the superiority of the second-moment turbulence model over eddy-viscosity one. Also, the further improvements of both turbulence models are discussed in order to overcome the discrepancy found between experimental and numerical data.

Introduction

Turbulent free flows occur in many practical situations. Also, some flows which are not considered to be free flows, *i. e.*, flames issuing from the burners in large furnaces, as a meter of fact, are the free flows. Problems of modeling free flames, and jets at all, arise because of the nonexistence of sharp edges of the physical fields. Also, it is impossibe to control the flow, based on the total mass balance.

The lowest level of modeling free premixed flame, offering any promise of realism, must, in some sense, account a transport of turbulent properties. The lowest level to do this is to use eddy-viscosity models, of which the k-ε variant is the most widely used. The present paper focuses on the use of two approaches to predict the turbulent stresses and fluxes, namely two-equations k-ε model and the full second-moment model.

The two-equations k-ε model is related to the turbulence energy, k, and its rate of dissipation, ε, both obtained from transport equations. Apart from accounting for turbulent transport, the eddy-viscosity approach offers the advantages of relative simplicity, and numerical stability. However, the main disadvantages of k-ε model are caused by

assumption that there is no vector space orientation for eddies, and by defining the turbulence length-scale using scalar variable. These disadvantages are specially manifested in the case of free axisymmetrical jets.

In order to overcome the imperfection of the eddy-viscosity concept we have used also the second-moment model. It allows both the transport and different development of the individual Reynolds stresses and scalar fluxes. Also, it has the advantage that terms accounting for anisotropy effects are introduced automatically into the transport equations. The generation rates of stresses, arising from the interaction between stresses and strains, do not need to be approximated. The significance of this fact may be inferred from the observation that, to a first approximation, the stress levels are given by:

$$\overline{u_i u_j} - \frac{2}{3} k\delta_{ij} = \text{turbulent time scale} \times \left(\frac{2}{3} G_{ij} - \delta_{ij} G_{kk} \right) \tag{1}$$

in which the left-hand side is the stress anisotropy while the right-hand-side bracket contains the anisotropy of stress generation. Of course, accuracy of the time scale determination remains a weak point even in the most advanced model variants formulated up to this time. Also, the above expression is used only for a particular simple model in order to deseribe the isotropy-promoting pressure-strain term in the stress-transport equations. The expression comes from intuition but carry out also an important message of principle.

In three dimensional space, the full second-moment model consists, of six transport equations for the Reynolds stresses. Additional transport equations for the turbulent fluxes of each scalar property, such as sensitive enthalpy and mass concentration of related species, have to be solved. Also, there is one extra transport equation for the dissipation rate of turbulence energy. The solution of all these complex equations together with those of mean flow is not a trivial task, and it is also computational expensive. In addition, there is considerable numerical difficulties arising from the use of second-moment model. The stabilizing effects of an eddy-viscosity field are absent in the mean-flow equations. Thus, although a second-moment model can provide a more realistic and rigorous approach for complex flow, such as premixed turbulent free acetylene flame, it is expensive with storage and execution time.

The main flow and structure of acetylene flame - turbulent field

The complexity of mathematical modeling of the free acetylene flame can be illustrated by the experimentally obtained flow field [1, 28]. At the same time, pinpointing some specific features of the mean flow and turbulent fields can be useful for further comparisons of the experimental data and calculated quantities. The flow field of the acetylene flame has four characteristic regions: central core (I); region having a constant width and very low entrainment of the surrounding air into the flame (II); transition region (III) and fully developed jet region (IV), (Fig. 1). Division into these four regions

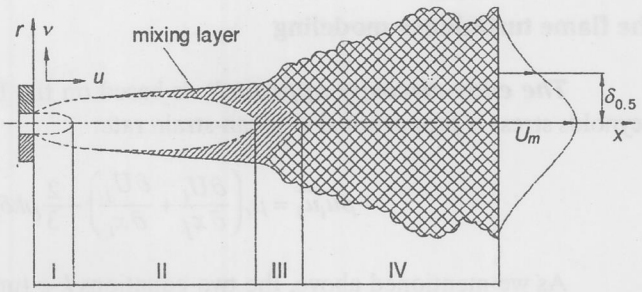

Figure 1. Free acetylene flame scheme

is based on the characteristic changes of the mean velocity and turbulence intensity at the flame axis [28].

The experimental observations suggest several specific properties of the premixed flame that pose characteristic and complex requirements to the mathematical model. Heat generation in the narrow region of the flame front causes sharp flow acceleration perpendicular to the flame front, that means in the radial direction, leading to the sharp increase in the turbulence intensity. The turbulent field in that region is very anisotropic because the flow acceleration and turbulence intensity increase are greater in the radial direction than in the axial direction. This can be seen from mean velocity and turbulence intensity profiles in the cross sections. The molecular viscosity increasing, turbulence intensity decreasing and flow relaminarization are caused by temperature increase in the flame front. Also, at the flame boundaries, the decreasing of the entrainment rate of the surrounding air into the flame is caused by drastic decreasing of the mixing intensity.

Small mixing intensity leads to the constant flame width in region II. Fully developed flame region is separated from the potential core by the region of the constant width and the transition region and starts at the distance $x/D = 25$ from the nozzle outlet. This distance for an isothermal jet is only $x/D = 5$–7. With the increase of the "fuel" to "air" ratio, relaminarization rate is greater, and the region of the constant fluid velocity is longer, leading to greater distance of the fully developed flame region from the nozzle outlet.

The mean velocity field of the free turbulent flow is described by the system of equations derived from Reynolds equations for stationary turbulent flow:

$$\frac{\partial}{\partial x_j}(\rho U_i U_j) = -\frac{\partial P}{\partial x_i} + \frac{\partial}{\partial x_j}\left[\mu\frac{\partial U_i}{\partial x_j} - \rho\overline{u_i u_j}\right], \quad \frac{\partial}{\partial x_j}(\rho U_j) = 0 \tag{2}$$

using the Reynolds decomposition of instantaneous velocity $\tilde{u}_i$ into a mean flow U_i and velocity fluctuations u_i, such that: $\tilde{u} = U_i + u_i$

Closure of the system of Reynolds momentum and continuity equations (2) for stationary turbulent flow of incompressible fluid has been done by using turbulence model transport equations.

The flame turbulence modeling

The eddy-viscosity approach is based on the Boussinesq assumption that Reynolds stress is proportional to mean-strain rate:

$$-\rho\overline{u_i u_j} = \mu_t\left(\frac{\partial U_i}{\partial x_j}+\frac{\partial U_j}{\partial x_i}\right)-\frac{2}{3}\rho k\delta_{ij} \tag{3}$$

As we mentioned above, the two-equations k-ε turbulent model was used [4]. The modeled transport equations of turbulent kinetic energy and its dissipation rate are:

$$U_j\frac{\partial k}{\partial x_j}-\frac{\partial}{\partial x_i}\left(\nu+\frac{\nu_t}{\sigma_k}\frac{\partial k}{\partial x_j}\right)=G-C_D\varepsilon \tag{4}$$

$$U_j\frac{\partial \varepsilon}{\partial x_j}-\frac{\partial}{\partial x_i}\left(\nu+\frac{\nu_t}{\sigma_\varepsilon}\frac{\partial \varepsilon}{\partial x_j}\right)=C_{\varepsilon 1}\frac{\varepsilon}{k}G-C_{\varepsilon 2}\frac{\varepsilon^2}{k} \tag{5}$$

where G is the production rate of k by shear forces. It is calculated from:

$$G=\nu_t\left(\frac{\partial U_i}{\partial U_j}+\frac{\partial U_j}{\partial U_i}\right)\frac{\partial U_i}{\partial U_j} \tag{6}$$

while the eddy-viscosity is described by: $\nu_t = C_\mu k^2/\varepsilon$

The standard two-equations k-ε model for free flows has shown adequate prediction of the two-dimensional plane jet development and significant disagreement in prediction of the axisymetric jet. Even 40% greater rate of spread of the axisymetric jet has been obtained [5]. Explanations for these disagreements have been searched for in the correlation analysis of two-dimensional plane and axisymetric jets [6]. It has been shown that the cross section of the large eddies depends on the width of flow field. The coherence of the large eddies in the axisymetric flow is weaker than in the plane flow. The last mentioned fact can be explained by the different rate of decay of characteristic velocity scale [7].

In the past, many efforts have been made in order to obtain the two-equations k-ε model that can be employed for the axisymetric jet and to remove described axisimetric/plane jets anomaly. One of these deserved to be highlighted. That is correlation proposed by Rodi [5] between of $C_{\varepsilon 1}$ and the jet spread coefficient β, defined as:

$$\beta=\left(\frac{\delta_{0.5}}{U_m}\right)\left(\frac{dU_m}{dx_l}\right) \tag{7}$$

$$C_{\varepsilon 1} = 1.14-5.31\beta \tag{8}$$

where: $\delta_{0.5}$ is the radial width of the jet where $U = 0.5\,U_m$, and U_m is the axial velocity at the symmetry axis (x_l) of the flow. This correction enabled the agreement of the calcula-

After some algebra, an equation is obtained for the correlations $\overline{u_i u_j}$, which for stationary flow has the form:

$$\overbrace{U_k \frac{\partial}{\partial x_k}\overline{u_i u_j}}^{C_{ij}} = -\overbrace{\left(\overline{u_j u_k}\frac{\partial U_i}{\partial x_k} + \overline{u_i u_k}\frac{\partial U_j}{\partial x_k}\right)}^{G_{ij}} + \overbrace{\frac{\partial}{\partial x_k}\left(\nu \frac{\partial \overline{u_i u_j}}{\partial x_k}\right)}^{T_{ij}} - \overbrace{2\nu\overline{\frac{\partial u_i}{\partial x_k}\frac{\partial u_j}{\partial x_k}}}^{E_{ij}} + \underbrace{\overline{\frac{p}{\rho}\left(\frac{\partial u_i}{\partial x_j} + \frac{\partial u_j}{\partial x_i}\right)}}_{\Phi_{ij}} - \underbrace{\frac{\partial}{\partial x_k}\left[\overline{u_i u_j u_k} + \overline{\frac{p}{\rho}(\delta_{jk}u_i + \delta_{ik}u_j)}\right]}_{\mathcal{D}_{ij}} \tag{11}$$

or:

$$C_{ij} = G_{ij} + T_{ij} + E_{ij} + \Phi_{ij} + \mathcal{D}_{ij} \tag{12}$$

The various groups of terms contributing to the stress balance are associated with different physical processes: C_{ij} identifies convection, G_{ij} represents production due to main flow deformations, T_{ij} denotes viscous molecular diffusion, E_{ij} represents dissipation by viscous processes, Φ_{ij} is the redistribution term caused by interaction between components of stress (interactions of pressure and flow deformations), and $\mathcal{D}_{ij}$ represents diffusion transport of turbulent stress components. Terms C_{ij}, G_{ij} and T_{ij} are used in their exact form, while terms E_{ij}, Φ_{ij} and $\mathcal{D}_{ij}$ have to be modeled.

Dissipation term E_{ij}. Dissipation processes are associated with the viscous effects inside the smallest scales of turbulent motion. At high Reynolds numbers, these scales are two or four orders of magnitude smaller than the largest, energy containing eddies that primarily interact with the mean strain. The general view is that turbulence energy "cascades" down along the eddy-size range. A little "leakage" occurring at intermediate scales. Turbulence energy ultimately is dissipated by the smallest eddies that are oblivious to the orientation of the mean flow and the large scales, thus being isotropic.

If the concept of isotropy of dissipation is accepted, it follows that all normal stresses are dissipated at a uniform rate, while shear stresses remain unaffected. Viscous destruction of $\overline{u_i u_j}$ is accordingly modeled by:

$$E_{ij} = -\frac{2}{3}\delta_{ij}\varepsilon \tag{13}$$

where $\varepsilon = \nu\overline{(\partial u_i/\partial x_k)^2}$, has to be determined.

Redistribution term Φ_{ij}. The pressure-strain term Φ_{ij} acts to redistribute energy among the normal stresses and to reduce shear stresses. This term, which tends to make the turbulence more isotropic, is modeled as the sum of two contributions, as follows:

$$\Phi_{ij} = \Phi_{ij,1} + \Phi_{ij,2} \tag{14}$$

where $\Phi_{ij,1}$ is the non-linear turbulent part, and $\Phi_{ij,2}$ is the mean-strain, or "rapid" part. $\Phi_{ij,1}$ and $\Phi_{ij,2}$ can be modeled by using the isotropisation-of-production assumptions [14]:

$$\Phi_{ij,1} = -C_1 \frac{\varepsilon}{k}\left(\overline{u_i u_j} - \frac{2}{3}\delta_{ij}k\right) \tag{15}$$

and

$$\Phi_{ij,2} = -C_2\left(G_{ij} - \frac{1}{3}\delta_{ij}G_{kk}\right) \tag{16}$$

where C_1 and C_2 are empirical constants. However, there are different proposals for modeling $\Phi_{ij,2}$. Gibson and Younis [15] also use (15) and (16) for Φ_{ij} but with different values of C_1 and C_2. The closure model of Launder-Reece-Rodi [13] uses (15) for $\Phi_{ij,1}$, and the following model for $\Phi_{ij,2}$ by using the quasi-isotropic assumptions:

$$\Phi_{ij,2} = -\alpha\left(G_{ij} - \frac{2}{3}\delta_{ij}G\right) - \beta\left(D_{ij} - \frac{2}{3}\delta_{ij}G\right) - \gamma k\left(\frac{\partial U_i}{\partial x_j} + \frac{\partial U_j}{\partial x_i}\right) \tag{17}$$

where $k = \overline{u_k u_k}/2$ is kinetic energy of turbulence, $G = G_{kk}/2$ is production of turbulent kinetic energy, and G_{ij} and D_{ij} are defined as follows:

$$G_{ij} = -\left(\overline{u_i u_k}\frac{\partial U_j}{\partial x_k} + \overline{u_j u_k}\frac{\partial U_i}{\partial x_k}\right) \tag{18}$$

$$D_{ij} = -\left(\overline{u_i u_k}\frac{\partial U_k}{\partial x_i} + \overline{u_j u_k}\frac{\partial U_k}{\partial x_j}\right) \tag{19}$$

We have used more complex quasi-isotropic model for the pressure-strain suggested by Launder [13], [20], so the term Φ_{ij} is modeled as follows:

$$\Phi_{ij} = -C_1\frac{\varepsilon}{k}\left(\overline{u_i u_j} - \frac{2}{3}\delta_{ij}k\right) - \alpha\left(G_{ij} - \frac{2}{3}\delta_{ij}G\right) -$$
$$-\beta\left(D_{ij} - \frac{2}{3}\delta_{ij}G\right) - \gamma k\left(\frac{\partial U_i}{\partial x_j} + \frac{\partial U_j}{\partial x_i}\right) \tag{20}$$

Coefficients α, β and γ are mutually dependent and are determined by coefficient C_2:

$$\alpha = \frac{8 + C_2}{11}; \quad \beta = \frac{8C_2 - 2}{11}; \quad \gamma = \frac{30C_2 - 2}{55} \tag{21}$$

Diffusion term $\mathcal{D}_{ij}$. Stress diffusion does not contribute greatly to the balance expressed by equation (11), except in regions of low stress production by mean strains, in which case diffusion is called upon to balance dissipation or pressure-strain processes. A certain degree of latitude can be exercised, therefore, in modeling diffusion without inflicting significant damage to the closure as a whole. Lumley [16] has provided arguments that indicate that the contribution of the pressure-velocity correlation to diffusion is sub-ordinate to that of triple correlation. A rational approach to modeling the latter group emerges upon the derivation of exact transport equations for $\overline{u_i u_j u_k}$. It is proposed that the triple correlations are governed by a balance between the rate of production and redistribution processes. Such arguments lead to:

$$\overline{u_i u_j u_k} = -C_s \frac{k}{\varepsilon}\left(\overline{u_i u_l}\frac{\partial \overline{u_j u_k}}{\partial x_l} + \overline{u_j u_l}\frac{\partial \overline{u_k u_i}}{\partial x_l} + \overline{u_k u_l}\frac{\partial \overline{u_i u_j}}{\partial x_l}\right) \tag{22}$$

However, it is held that diffusion contribute little the overall stress balance, and that the symmetry in implicit approximation (22) is not consistent with the asymmetry. A simpler form of (22) [17], which includes only the first of the three bracketed terms, has been preferred whenever calculations for complex flow have included stress transport effects. Thus:

$$\mathcal{D}_{ij} = -C_s \frac{\partial}{\partial x_k}\left(\frac{k}{\varepsilon}\overline{u_k u_l}\frac{\partial \overline{u_i u_j}}{\partial x_l}\right) \tag{23}$$

Rate of turbulent kinetic energy dissipation ε. There remains the task to determine ε. An exact transport equation for ε can be derived [18], but is not useful as basis for modeling, for it contains many obscure terms correlating small-scale processes. The modeling route is preferably based on the cascade concept and focuses on large-scale processes in precisely the same way as it is done in the case of the k-ε eddy-viscosity model. Indeed, the equation used in the large majority of second-moment model calculations of high-Reynolds-number flows is a variant of the equation (5) used in the k-ε model, namely:

$$U_j \frac{\partial \varepsilon}{\partial x_j} = \frac{\partial}{\partial x_i}\left[\left(\nu + C_\varepsilon \frac{k}{\varepsilon}\overline{u_i u_j}\right)\frac{\partial \varepsilon}{\partial x_j}\right] + C_{\varepsilon 1}\frac{\varepsilon}{k}G - C_{\varepsilon 2}\frac{\varepsilon^2}{k} \tag{24}$$

the main difference being the use of the tensorial "diffusivity" instead of $C_\mu k^2/\sigma_\varepsilon \varepsilon$, introduced in equation (5).

Model has six constants, the values of which have been proposed based on the experimental data and numerical optimization:

C_1	C_2	C_s	$C_{\varepsilon 1}$	$C_{\varepsilon 2}$	C_ε
1.5	0.4	0.22	1.45	1.9	0.15

The concentration and temperature fields model

The model encompasses conservation equations of gas components participating in the process (C_2H_2, O_2, N_2, CO_2, H_2O) and energy equation. To deal with chemical reactions we have solved conservation equations of participating specie. Equation for mass fraction of species "A", Y_A have general form:

$$U_k \frac{\partial Y_A}{\partial x_k} = -\frac{\partial}{\partial x_k}\overline{u_k y_A} + \frac{\partial}{\partial x_k}\left(\mathcal{D}_A \frac{\partial Y_A}{\partial x_k}\right) + \dot{\Omega}_A \tag{25}$$

The equations have been closed by means of conservation equations for Reynolds fluxes $\rho\overline{u_i y}$ that are of the modeled form:

$$U_k \frac{\partial}{\partial x_k}\overline{u_i y} = -\left(\overline{u_k u_i}\frac{\partial Y}{\partial x_k} + \overline{u_k y}\frac{\partial U_i}{\partial x_k}\right) - \left(C_{y1}\frac{\varepsilon}{k}\overline{u_i y} - C_{y2}\overline{u_k y}\frac{\partial U_i}{\partial x_k}\right) +$$

$$+\frac{\partial}{\partial x_j}\left[C_s\frac{k^2}{\varepsilon}\left(\frac{\partial \overline{u_i y}}{\partial x_j} + \frac{\partial \overline{u_j y}}{\partial x_i}\right)\right] + \frac{\partial}{\partial x_j}\left(\frac{\nu}{\sigma_y}\frac{\partial}{\partial x_j}\overline{u_i y}\right) + S_y \qquad (26)$$

where: $S_y = \overline{u_i \dot{\omega}} = -C_\omega \frac{k}{\varepsilon}\overline{u_i u_j}\frac{\partial \dot{\Omega}_A}{\partial x_j}$, and $C_{y1} = 3.3$, $C_{y2} = 0.4$, $C_s = 0.15$.

Production and destruction of particular components in the mixture are shown as part of the source terms of the equations, through the kinetic relations and corresponding stoichiometric ratios. Basic chemical equation of acetylene combustion is as follows: $C_2H_2 + 2.5O_2 = 2CO_2 + H_2O + H_{cr}$, where $H_{cr} = 1.2 \cdot 10^6$ kJ/kmol is the heat effect of chemical reaction.

Heat transfer in the flame was considered through the equation of sensitive enthalpy $h_s = \Sigma_l Y_l c_{p,l} T$. Enthalpy equation has the same form as equation (25), but with source term equal:

$$S_h = U_k \frac{\partial P}{\partial x_k} + q_r + \dot{\Omega}_{C_2H_2} H_{cr} \qquad (27)$$

where term $\dot{\Omega}_{C_2H_2} H_{cr}$ describes the heat effect of the chemical reaction in the flame. The term q_r on the right hand side of the equation (27) represents the heat source due to the radiation.

For the radiation heat transfer six flux model [19] is reduced, for axial-symmetric case of purely emission-absorption radiation, to two-equation model. The diffusion type expressions for radiation fluxes, in axial ($R_x = I_x + J_x$) and radial ($R_r = I_r + J_r$) directions were used:

$$\frac{\partial}{\partial x}\left(\frac{I}{k_a}\frac{\partial R_x}{\partial x}\right) = K_a R_x - \frac{1}{3}K_a I_b, \quad \frac{1}{r}\frac{\partial}{\partial r}\left(\frac{1}{k_a} r \frac{\partial R_r}{\partial r}\right) = K_a R_r - \frac{1}{3}K_a I_b \qquad (28)$$

where I_b is the emission power of the black body, and $K_a = -(1/L)\ln(1 - e_g)$ is the absorption coefficient of the medium. In the energy equation, the heat source due to the radiation is described by the term:

$$q_r = \mathrm{div}\vec{Q}_r = K_a\left(R_x + R_r - \frac{2}{3}I_b\right) \qquad (29)$$

Reynolds fluxes $\overline{\rho u_i h_s}$ are modeled in same way as $\overline{\rho u_i y}$ in the equation (26).

The combustion model

Determination of adequate term for the average combustion rate $\dot{\Omega}_A$ that appears in equations (25–27), is the second basic problem concerning the free turbulent flame. However, this paper is mostly dealing with turbulence models, so it was paid less

attention to the combustion rate model. Several different models proposed to determine real combustion rates have been reviewed in *e. g.* [24].

Generally speaking, two facts complicate the determination of the combustion rate. First, a great number of intermediate species has been identified in combustion of the typical hydrocarbon fuel. Any attempt to simulate anything like all the corresponding intermediate reactions would arouse large computational difficulties. Second, because of highly nonlinear dependence of combustion rate on temperature, the determination of the time-averaged value is far from straightforward.

Concerning the first difficulty, it is fortunate that the all important heat release can be determined by supposing a one-step global reaction leading to carbon dioxide and water. For practical purposes, this assumption is used in this work. Some slight improvement is probably possible by supposing a two-step reaction of the following kind. The first step yielding to CO and H_2, is rapid, and reaction rate is controlled by the turbulent mixing. The subsequent conversion of the CO occurs in the well-mixed product "packets" from the first step and combustion rate is controlled by CO reaction with the hydroxyl radical. The conversion of hydrogen is rapid and governed by availability of oxygen.

The second difficulty is avoided by expanding the Arrhenius combustion term in a truncated series and then deriving modeled equations for the turbulence correlations that arise out of the time-averaging. This approach suffers from two major disadvantages. First, the retention of sufficient terms in the series expansion results in an uneconomic number of correlation equations that has to be solved. Second, the modeled equations for these correlations are very difficult to validate.

The alternative rout to obtain the combustion rate based on the chemical kinetic, is to use the approximated Arrhenius relation [27], which for acetylene oxidation is:

$$\dot{\Omega}_{ck} = A Y_{C_2H_2}^{0.5} Y_{O_2}^{1.25} \rho^{1.75} \exp\left(-\frac{E}{RT}\right) \tag{30}$$

where $A = 9.5 \cdot 10^{11}$ and $E/R = 1.51 \cdot 10^4\ \mathrm{K}^{-1}$. The obtained combustion rate is much greater than combustion rate in the real flame.

The more effective way to circumvent the second difficulty is contained in the fact that the time scale of the turbulence decay is typically much longer than the chemical kinetic time scale. Practically, all the combustion occurs after mixing between the small scale dissipative eddies. We cannot make to large error by ignoring the kinetic rate of the overall reaction and linking the combustion rate to the turbulence decay rate.

In this paper, the model of combustion rate was based on the originally "Eddy-Break-Up" model, proposed by Spalding [30, 31]. According to this model, it was assumed that the combustion reactions are controlled by the rate of turbulence production destruction, which is characterized by the turbulence time scale of large eddies, $\tau = k/\varepsilon$. Fuel and oxidant concentrations appear as the limiting factors, and thus:

$$\dot{\Omega}_{\tau} = A_{C_2H_2} \rho \frac{\varepsilon}{k} \min\left| Y_{C_2H_2}, \frac{Y_{O_2}}{s} \right| \tag{31}$$

Coefficient $A_{C_2H_2}$ has a universal value of 0.53 [11], and s is the stoichiometric ratio of the fuel and oxidant. In domain of lower temperatures, the rate is controlled by the chemical reaction kinetics, so the combustion rate was determined as follows:

$$\dot{\Omega}_{C_2H_2} = \min(\dot{\Omega}_{ck}, \dot{\Omega}_{\tau}) \tag{32}$$

The computational details

The complete mathematical model with eddy-viscosity approach is standard one, but with described corrections, given in reference [3]. The second-moment model described in the previous paragraphs consists of a set of differential equations equal in number to the following list of unknowns: the axial and radial velocity components U, V, pressure P; temperature T; mass concentration of related species: $Y_{C_2H_2}$, Y_{O_2}, Y_{N_2}, Y_{CO_2}, Y_{H_2O}; velocity variances: $\overline{uu}, \overline{vv}, \overline{ww}, \overline{uv}$; rate of turbulent kinetic energy dissipation ε, related scalar variances: $\overline{ut}, \overline{vt}, \overline{uy_{C_2H_2}}, \overline{vy_{C_2H_2}}, \overline{uy_{O_2}}, \overline{vy_{O_2}}, \overline{uy_{N_2}}, \overline{vy_{N_2}}, \overline{uy_{CO_2}}, \overline{vy_{CO_2}}, \overline{uy_{H_2O}}, \overline{vy_{H_2O}}$, and total axial and radial radiation fluxes R_x, R_r. It should be noted that variance $\overline{ww}$ must be solved in second order closure equations and cylindrical-polar coordinate frame, in spite of two-dimensional problem. The equations written in cylindrical-polar coordinate frame have the general form:

$$\frac{\partial}{\partial x}(\rho U\Phi) + \frac{1}{r}\frac{\partial}{\partial r}(r\rho V\Phi) = \frac{\partial}{\partial x}(\Gamma_\Phi \frac{\partial \Phi}{\partial x}) + \frac{1}{r}\frac{\partial}{\partial r}(r\Gamma_\Phi \frac{\partial \Phi}{\partial r}) + S_\Phi \tag{33}$$

where Φ is any of the above dependent variables, and Γ_Φ and S_Φ are related transport coefficients and the source terms for any particular variables Φ. Physical properties of the mixture are obtained by the auxiliary thermodynamic relations. Special attention was paid to the boundary conditions which should be posed in the "quiescent" fluid, as it has been described by details in reference [2].

The equations are solved by the finite-volume procedure based on SIMPLE algorithm [32, 33] and embodied in a version of the TEACH-T computer code adopted for this purpose. The non-uniform numerical grid with 32 control nodes in radial and 45 in axial direction has been used for computations.

The computational results

The verifications of the models were performed by comparing the numerical results with the measuremens of the mean axial and radial velocity and turbulence intensity fields in the acetylene flame carried on by using laser anemometry [1, 29]. Also, calculated flame mean temperatures were compared with the experimental results in temperature range that could be measured by the thermocouples [1]. Attention has also been paid to the deeper insight into the turbulence structure obtained by second-moment model.

Fig. 2 shows the experimental data and computation results for the axial mean velocity change along the flame axis using k-ε model (Fig. 2a), and second-moment model (Fig. 2b). Experimental evidence shows, that in region $x/D < 5$, temperature increases, *e. g.* density decreases. Velocity increase due to the gas expansion is dominant compared to the flow deceleration due to the shear stresses at the front of the flame, leading to the acceleration of the flame jet in this region. Evidently, this effect is captured by second-moment model (Fig. 2b), nevertheless, less pronounced in the model than in the experimental data. It must be pointed out that this effect could not be obtained by eddy-viscosity model (Fig. 2a). Once it begins, temperature decrease in the flame helps the velocity decrease along the jet axis in region $x/D > 5$. Also, it is evident that agreement between numerical and experimental data in this region is much better in second-moment model then in k-ε model. Excess air in the premixed mixture may be used to influence the position of the region of velocity decrease. The mixture richer in fuel yields higher temperatures and the slower velocity decrease. Velocity change along the flame axis is also influenced by the exit velocity values at the nozzle outlet. High exit velocity at the nozzle outlet causes wider flame front, probably due to the dependence of the flame spreading rate on the velocity of the incoming gas flow. The mentioned influences on the flow characteristics of the flame are hard to express quantitatively, since every flame is unique in its own.

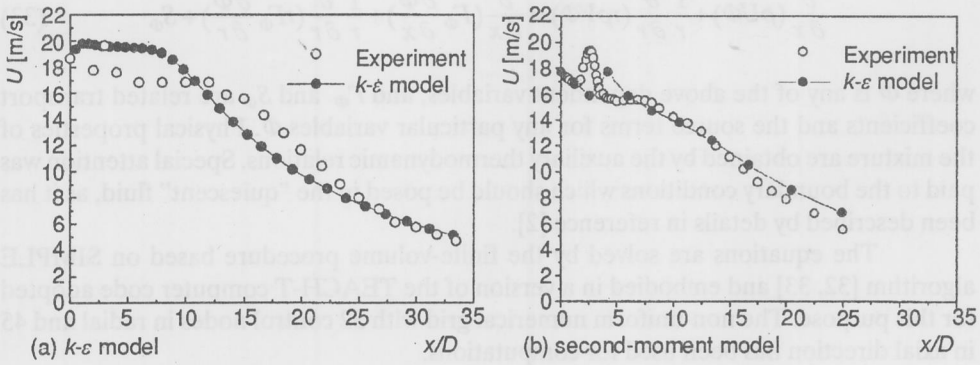

Figure 2. Mean velocity along the flame axis

On Fig. 3, computed radial mean velocity profiles are shown at different axial locations. Radial velocity profiles, obtained by both models and experiment, become similar to the common shape profile at ten diameters downstream. Such behavior was expected due to the self-preservation of turbulence in fully developed region. Experimentally determined radial velocity profiles [1, 28] in the shape of the saddle at the cross-sections near the nozzle outlet have not been adequately reproduced by the models.

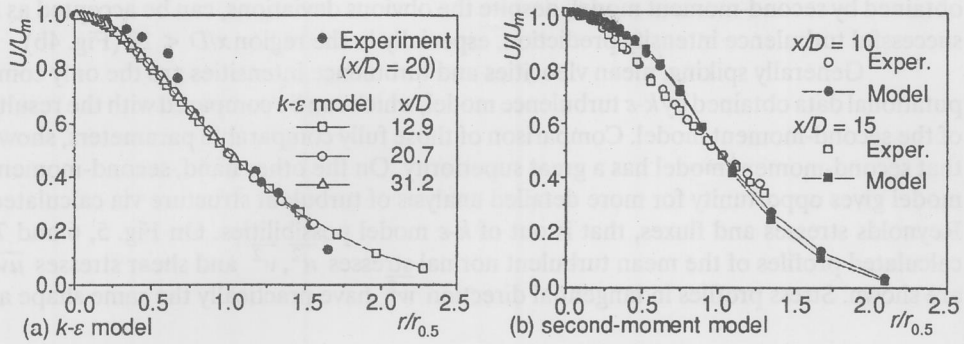

Figure 3. Radial profiles of axial mean velocity

A similar situation has been obtained for the plane jet [5] and explained by the inability of the models to encompass the secondary flows in the plane perpendicular to the jet axis.

The comparisons of the experimentally obtained and calculated parameters of the flame flow field have also been made for turbulence intensity along the flame axis, $u_{rms} = \sqrt{\overline{uu}}$, (Fig. 4). It has to be noticed that variance $\overline{uu}$ is calculated from:

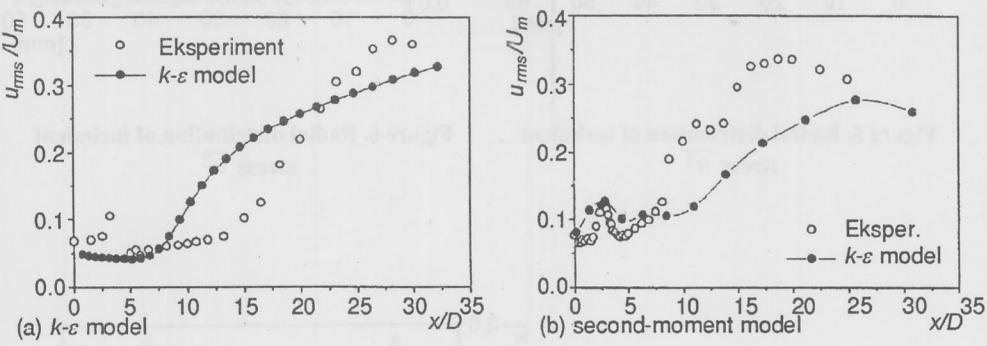

Figure 4. Turbulence intensity along flame axis

$$\frac{\overline{uu}}{k} = \frac{2}{3}\left[1 + \frac{0.8}{1 + \frac{\rho\varepsilon}{G}}\right]$$

in case of k-ε model, and that in case of second-moment model it was obtained from its transport equation. Considering the complexity of the problem, computation results

obtained by second-moment model, despite the obvious deviations, can be accepted as a successful turbulence intensity prediction, especially in the region $x/D < 10$ (Fig. 4b).

Generally spiking, mean vleocities and turbulence intensities are the only computational data obtained by k-ε turbulence model, which can be compared with the results of the second-moment model. Comparison of those fully comparable parameters, shows that second-moment model has a great superiority. On the other hand, second-moment model gives opportunity for more detailed analysis of turbulent structure via calculated Reynolds stresses and fluxes, that is out of k-ε model possibilities. On Fig. 5, 6 and 7, calculated profiles of the mean turbulent normal stresses $\overline{u^2}, \overline{v^2}$ and shear stresses $\overline{uv}$ are shown. Stress profiles in tangential direction $\overline{w^2}$ have practically the same shape as

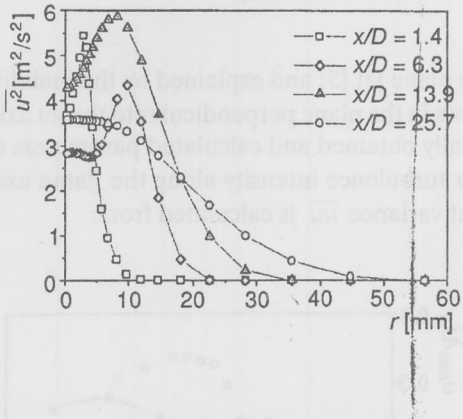

Figure 5. Radial distribution of turbulent stress $\overline{u^2}$

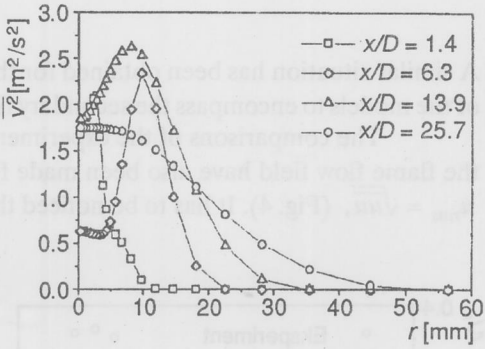

Figure 6. Radial distribution of turbulent stress $\overline{v^2}$

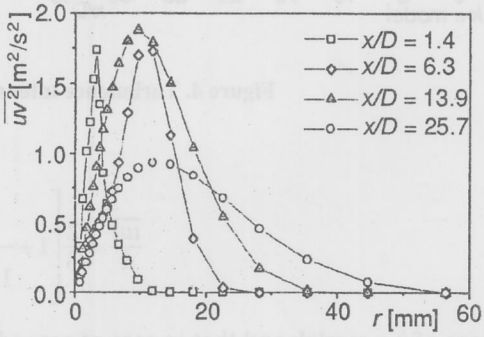

Figure 7. Radial distribution of turbulent shear stress $\overline{uv}$

the $\overline{v^2}$, with approximately 20% higher values. Figures 5, 6 and 7 show the level and anisotropy of turbulence in particular regions of the flame, and can be used for more detailed theoretical analysis of the transport processes in the flame. With the same aim on Fig. 11, 12 and 14, radial profiles of turbulent fluxes $\overline{uy_i}$, $\overline{vy_i}$, $\overline{ut}$ and $\overline{vt}$ are shown.

In Fig. 8, change of the mass concentrations of the chemical components along the flame axis have been shown. To illustrate combustion process, on Fig. 9 and 10, calculated radial profiles of carbon dioxide and oxygen mass concentrations at particular axial locations are shown, respectively. From these figures, the extension of the flame front in radial direction, as well as, entraiment of the fresh air in the jet beyond the flame

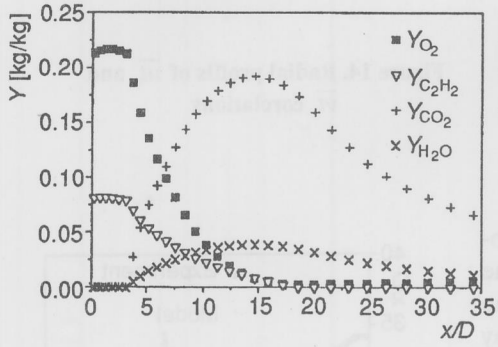

Figure 8. Radial distribution of active species concentration Y_A

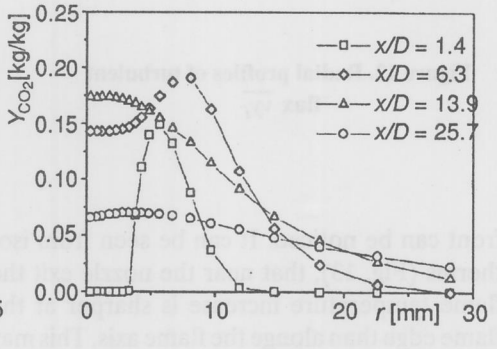

Figure 9. Development of the CO_2 concentration profile

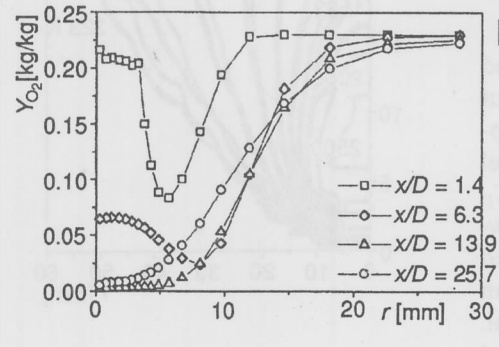

Figure 10. Development of the O_2 concentration profile

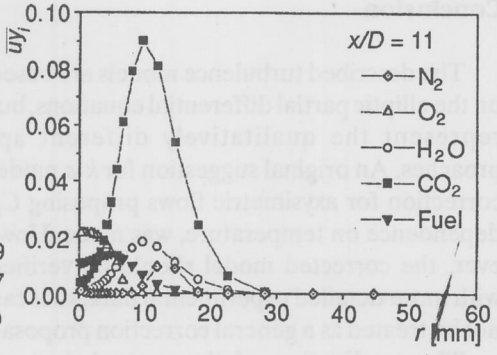

Figure 11. Radial profiles of turbulent flux $\overline{uy_i}$

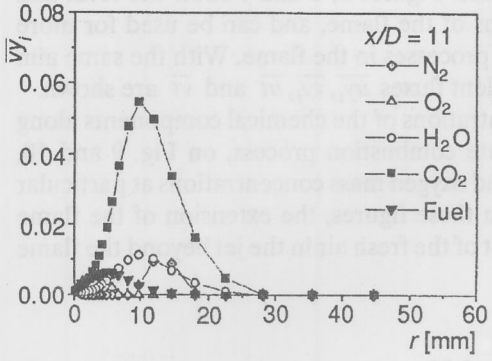

Figure 12. Radial profiles of turbulent flux $\overline{vy_i}$

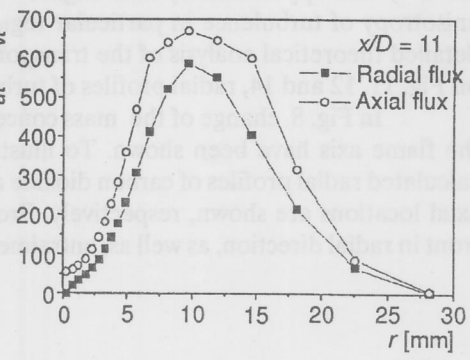

Figure 14. Radial profils of $\overline{ut}$ and $\overline{vt}$ corelations

front can be noticed. It can be seen from isotherms (Fig. 13), that near the nozzle exit the flame temperature increase is sharper at the flame edge than alonge the flame axis. This may seem unexpected. But, it can be explained by the violent reaction with oxidant in excess at the flame edge, and by the longer reaction time due to the lower velocities in this region.

Conclusion

The described turbulence models are based on the elliptic partial differential equations, but represent the qualitatively different approaches. An original suggestion for k-ε model correction for axysimetric flows proposing C_D dependence on temperature, was made. However, the corrected model should be verified with more detailed experimental data, so it can not be treated as a general correction proposal.

The application of the second-moment model provides a powerful tool for improving the prediction accuracy of premixed free flames. As it is demonstrated by comparing of

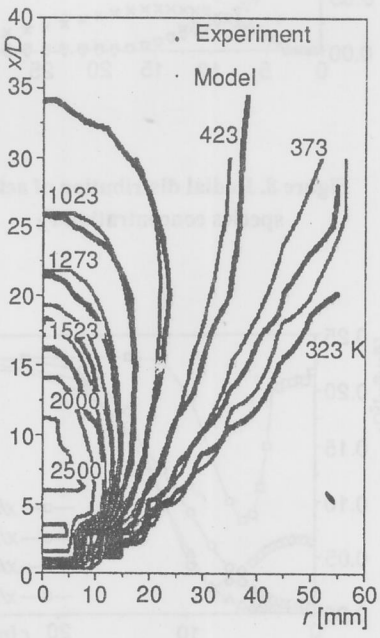

Figure 13. Contours of flame temperature

the numerical and experimental results, the modeling of observed anisotropy levels and correlation coefficient must be carried out with special care. The model provides insight into the structure and aerodynamic characteristics of the flame.

The problem of modeling the free flames has only begun to be solved in this paper. First of all, the model should be verified with more detailed experimental data. A modern approach to the modeling of combustion requires attention to be paid to the turbulent density fluctuations. It means that the models have to be developed with Favre averaging or turbulent correlations with density fluctuations. Also, a more detailed analysis may be required for the modeling of the chemical reactions, especially formation of char in the flame.

Acknowledgments

Described research has been financed by the Ministry of Science and Technology of Serbia (grant 08M01).

Nomenclature

A [–] – combustion rate constant
C [–] – turbulence model coefficients
$\mathcal{D}_A$ – Reynols stress diffusion term
D [m] – orifice diameter
E – activation energy
e [–] – emissivity
H_{cr} – chemical reaction heat effect
h [J·kg^{-1}] – enthalpy
I, J [Wm^{-2}] – heat radiation intensity
k [m^{2}s^{-2}] – turbulent kinetic energy
L [m] – mean beam length
P [Nm^2] – mean static pressure
p – pressure fluctuations
q [Wm^2] – heat flux
Q [W] – heat flow rate
R – gas constant
R_x, R_r [Wm^{-2}] – total radiation fluxes
r [m] – radial coordinate
s [–] – stoichiometric ratio
T [K] – temperature
t [K] – fluctuating temperature
U_i [ms^{-1}] – mean velocity components, U, V
u_i [ms^{-1}] – fluctuating velocity components
x_i [m] – coordinates
Y_A [kg·kg^{-1}] – mass concentration of component A
yA [kg·kg^{-1}] – fluctuating mass concentration of component A

Greek symbols

α	– second-moment model constant
β	– jet spread coefficient, second-moment model constant
γ	– second-moment model constant
Γ	– transport coefficient
δ [m]	– jet width, where $U = U_m/2$
ε [m^2s^{-3}]	– rate of turbulent kinetic energy dissipation
μ [$kgm^{-1}s^{-1}$]	– dynamic viscosity
ν [m^2s^{-1}]	– kinematic viscosity
ρ [$kg \cdot m^{-3}$]	– density
Ω [$kg \cdot m^{-3}s^{-1}$]	– average combustion rate
$\dot{\omega}$ [$kg \cdot m^{-3}s^{-1}$]	– fluctuating part of combustion rate
Φ [varies]	– general dependent variable
τ [s]	– turbulence time scale
θ	– correction factor in k-ε model

Subscripts

a	– absorption
b	– black body
g	– gas
i, j, k, l	– tensor notation indices
t	– turbulent
r	– radial direction, or radiation
x	– axial direction

Superscripts

$\sim$	– instantaneous
$(-)$	– time-averaged

References

[1] Bakić, V., Investigation of a Turbulence Flame Structure Using Conditional Signal Sampling, MSc Thesis, University of Belgrade, Mech. Eng. Faculty, Yugoslavia, 1997

[2] Sijerčić, M., Nemoda, S., Bakić, V., Modeling of Turbulent Premixed Jet Flame by Means of Second Order Closure, Proceedings of the 2nd Int. Symposium on Turbulence, Heat and Mass Transfer, (Eds. K. Hanjalić, T.W.J. Peeters), Delft University Press, 1997, pp. 729–738

[3] Sijerčić, M., Oka, S., Turbulence Model for a Premixed Jet Flame, *Thermal Science, Int. issue of the Journal Termotehnika*, Belgrade, *10*, (1994), 3–4, pp. 153–170

[4] Launder, B. E., Spalding, D. B., The Numerical Computation of Turbulent Flows, *Comp. Meth. in Applied Mech. and Eng.*, North-Holand, *3* (1974), pp. 269–289

[5] Mc Guirk, J., Rodi, V., Calculation of the Threedimensional Turbulent Jets, in Turbulent Shear Flows (in Russian), Mashinostroenie, Moscow, pp. 72–88, 1982

[6] Gutmark, E., Wygnanski, I., The Planar Turbulent Jet, *J. Fluid Mech. 73* (1976), pp. 465–493

[7] Lockwood, F. C., Syed, S. A., Consideration of the Problem of Combustion Modeling for Engineering Application, *Combustion Science and Technology, 19* (1979), pp. 129–140

[8] Lockwood, F. C., Stolakis, P., Assessment of Two Turbulence Models for Turbulent Round Diffusion Jets with Combustion, *Proceedings* of the Fourth Symposium on Turbulent Shear Flows, Karlsruhe, Germany, 1983, pp. 10.25–10.31

[9] Patankar, S. V., Spalding, D. B., Heat and Mass Transfer in Boundary Layers, Intertext Books, London, 1970

[10] Ballal, D. R., Studies of Turbulent Flow - Flame Interaction, *AIAA J., 24* (1986), 1, pp. 1148–1154

[11] Glassman, I., Combustion, Academic Press, New York, 1987

[12] Hinze, J. O., Turbulence, McGraw Hill, 1975

[13] Launder, B. E., Reece, G. J., Rodi, W., Progress in the Development of a Reynolds Stress Turbulence Closure, *J. Fluid Mech., 68* part 3 (1975), pp. 537–566
[14] Gibson, M. M., Rodi, G., *J. Fluid Mech., 68* (1975), p. 537
[15] Gibson, M. M., Youns, B. A., Calculation on Swirling Jets with a Reynolds Stress Closure, *Physics Fluids, 29* (1986), p. 38
[16] Lumley, J. L., VKI Lecture Series 76, Prediction Methods for Turbulent Flows, Brussels, 1975
[17] Daley, B. J., Harlow, F. H., Transport Equations of Turbulence, *J. Physics Fluids, 13* (1970), p. 2634
[18] Tennekes, H., Lumley, J. L., A First Course in Turbulence, MIT Press, 1978
[19] Chu, T. C., Churchill, S. W., Numerical Solution of Problems in Multiple Scattering of Electromagnetic Radiation, *J. Phis. Chem., 59* (1955), pp. 855–863
[20] Launder, B. E., Second-Moment Closure: Methodology and Practice, in Colection de la Direction des Études et recherches d'Électricité de France, Paris, pp. 111–120, 1984
[21] Leschziner, M. A., Second-Moment Closure for Complex Flows, Int. Forum on Mathematical Modeling of Processes in Energy Systems, ICHMT, Sarajevo, 1989
[22] ***, Collaboration Testing of Turbulence Models, International Project Run from Stanford University, 1990–1992
[23] ***, Turbulent Reacting Flows (Eds. P. A., Libby, F. A., Williams), Academic Press, London, 1995
[24] Khalil, E. E., Modeling of Furnaces and Combustors, Abacus Press, London, 1982
[25] Byggstoyl, S., Magnussen, B. F., *Proceedings*, Fourth Symposium on Turbulent Shear Flows, Karlsruhe, (1983), pp. 10.32–10.38
[26] Driscoll, R., Kennedy, L., *Proceedings*, 19th Symposium (Internat.) on Combustion, Pittsburgh, Combustion Institute, (1982), pp. 387–392
[27] Essenigh, R. H., Suuberg,E. M., The Role of Volatiles in Coal Combustion, *Proceeding,* NATO Advanced Research Workshop on Fundamentals of the Physical Chemistry of Pulverized Coal Combustions, Les Ares, 1986
[28] Matović, M., Oka, S., Durst, F., Structure of the Velocity and Turbulent Field in Premixed Axisymmetric Flames, *Journal of Fluids Engineering, 116* (1994), pp. 631–642
[29] Sijerčić, M., Oka, S., Vujović, V., Contribution to the Modeling of the Axysimetric Turbulent Jets, (in Serbian) 20th YU Congress of Theoretical and Applied Mechanics, Kragujevac, pp. 157–160, 1993
[30] ***, Turbulent reacting flows (in Russian) (Eds. P., A., Lybby, F. A., Williams), "Mir", Moscow, 1983
[31] Spalding, D. B., Mathematical Models of Turbulent Flames; A Review, Combustion Science and Technology, *13* (1976) pp. 3–25
[32] Gosman, A. D., Pun, W.,P., Calculation of Recirculating Flows, Mech. Eng. Depart., Imperial College, London, 1973
[33] Patankar, V. S., Numerical Heat Transfer and Fluid Flow, McGraw-Hill, 1980

Authors address:
M. Sijerčić, Ž. Stevanović
Laboratory for Thermal Engineering and Energy
Vinča Institute of Nucelar Sciences, Belgrade, Yugoslavia
P. O. Box 522, 11001 Belgrade, Yugoslavia

Paper submited: December 18, 1997
Paper revised: April 29, 1998
Paper accepted: September 10, 1998